**LETTER TO THE EDITOR**

# Magnetic ordering in $Gd_2Sn_2O_7$: the archetypal Heisenberg pyrochlore antiferromagnet

**A S Wills,[1,2] M E Zhitomirsky,[3] B Canals,[4] J P Sanchez,[3] P Bonville,[5] P Dalmas de Réotier[3] and A Yaouanc[3]**

[1]Department of Chemistry, University College London, 20 Gordon Street, London, WC1H 0AJ, UK
[2]Davy-Faraday Research Laboratory, The Royal Institution of Great Britain, London W1S 4BS, UK
[3]Commissariat à l'Energie Atomique, DSM/DRFMC/SPSMS, 38054 Grenoble, France
[4]Laboratoire Louis Néel, CNRS, BP-166, 38042 Grenoble, France
[5]Commissariat à l'Energie Atomique, DSM/SPEC, 91191 Gif-sur-Yvette, France

**Abstract.** Low-temperature powder neutron diffraction measurements are performed in the ordered magnetic state of the pyrochlore antiferromagnet $Gd_2Sn_2O_7$. Symmetry analysis of the diffraction data indicates that this compound has the ground state predicted theoretically for a Heisenberg pyrochlore antiferromagnet with dipolar interactions. The difference in magnetic structures of $Gd_2Sn_2O_7$ and of nominally analogous $Gd_2Ti_2O_7$ is found to be determined by a specific type of third-neighbor superexchange interaction on the pyrochlore lattice between spins across empty hexagons.

Frustration or inability to simultaneously satisfy all independent interactions [1] has become an important theme in condensed matter research, coupling at the fundamental level a wide range of phenomena, such as high-$T_c$ superconductivity, the folding of proteins and neural networks. Magnetic crystals provide one of the simplest stages within which to explore the influence of frustration, particularly when it arises as a consequence of lattice geometry, rather than due to disorder. For this reason, geometrically frustrated magnetic materials have been the objects of intense scrutiny for over 20 years [2]. Particular interest has been focussed on *kagomé* and *pyrochlore* (see Fig. 1) geometries of vertex-sharing triangles and tetrahedra respectively. Model materials with their structures display a wide range of exotic low-temperature physics, such as spin ice [3], spin liquids [4], topological spin glasses [5], heavy fermion [6], and co-operative paramagnetic ground states [7]. Research into these systems was spawned from studies of the archetypal geometrically frustrated system—the Heisenberg pyrochlore antiferromagnet, which in the classical limit was shown theoretically to possess a disordered ground state. Raju and co-workers found that the Heisenberg pyrochlore antiferromagnet with dipolar interactions has an infinite number of degenerate spin configurations near the mean-field transition temperature, which are described by propagation vectors [*hhh*] [8]. Later, Palmer and Chalker showed that quartic terms in the free energy lift this degeneracy and stabilize a four-sublattice state with the ordering vector $\mathbf{k} = (0\,0\,0)$ (the PC state) [9].

Among various pyrochlore materials $Gd_2Ti_2O_7$ and $Gd_2Sn_2O_7$ are believed to be good realizations of Heisenberg antiferromagnets. Indeed, the $Gd^{3+}$ ion has a half-filled $4f$-shell with nominally no orbital moment. A strong *intrashell* spin-orbit

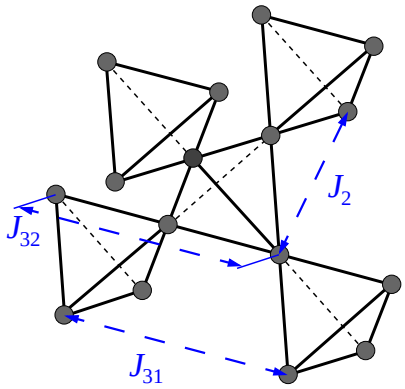


**Figure 1.** Pyrochlore lattice of vertex sharing tetrahedra. Next-neighbor exchanges are shown by long-dashed line.

coupling mixes, however, $^8S_{7/2}$ and $^6P_{7/2}$ states leading to a sizable crystal-field splitting. Recent ESR measurements on dilute systems gave comparable ratios of the single-ion anisotropy constant $D > 0$ to the nearest-neighbor exchange $J$ for the two compounds: $D/J \sim 0.7$ [10]. This corresponds to a planar anisotropy for the ground state. Magnetic properties of the stannate and the titanate would be expected, therefore, to be very similar. In this light, the contrasts between the low-temperature behavior of $Gd_2Sn_2O_7$ and that of the analogous titanate are remarkable. While the titanate displays two magnetic transitions, at $\sim 0.7$ and 1 K, to structures with the ordering vector $\mathbf{k} = \left(\frac{1}{2}\,\frac{1}{2}\,\frac{1}{2}\right)$ [11, 12], the stannate undergoes a first-order transition into an ordered state near 1 K [13]. Furthermore, Mössbauer measurements indicate that in the latter the correlated $Gd^{3+}$ moments still fluctuate as $T \to 0$ K [14].

In this article we demonstrate that $Gd_2Sn_2O_7$ orders with the PC ground state, evidencing it as an experimental realization of a Heisenberg pyrochlore antiferromagnet with dipolar interactions. We also note that the magnetic structure observed in $Gd_2Sn_2O_7$ differs from those observed in the closely related $Gd_2Ti_2O_7$, indicating that an extra interaction is at play in the latter which leads to the observed differences.

In order to reduce the absorption of neutrons, a 500 mg sample of $Gd_2Sn_2O_7$ enriched with $^{160}$Gd was prepared following conditions given in Ref. [13]. Powder neutron diffraction spectra were collected with neutrons of wavelength 2.4 Å using the D20 diffractometer of the ILL at two temperatures below $T_N$=1 K (0.1 K and 0.7 K), as well as one temperature in the paramagnetic phase above $T_N$ (1.4 K). Due to the high residual absorption of the Gd sample, extended counting times of 5 hours per temperature were required. The magnetic contribution to diffraction at 0.1 K could be well isolated from scattering by the cryostat walls and dilution insert by subtraction of the spectrum at 1.4 K. Symmetry calculations were made using SARA*h* [15] and Rietveld refinement of the diffraction data using Fullprof [16] together with SARA*h*.

The magnetic diffraction peaks, Fig. 2, can be indexed with the propagation vector $\mathbf{k} = (0\,0\,0)$. The different types of magnetic structure can be classified in terms of the irreducible corepresentations of the reducible magnetic corepresentation, $c\Gamma_{mag}$. In the case of $Gd_2Sn_2O_7$ (space group $Fd\bar{3}m$ with $\mathbf{k} = (0\,0\,0)$ and $Gd^{3+}$ ion at the 16*d* crystallographic position) this can be written: $c\Gamma_{mag} = 1c\Gamma_{3+} + 1c\Gamma_{5+} + 1c\Gamma_{7+} + 2c\Gamma_{9+}$ [17, 18]. Their associated basis vectors are represented in Fig. 3. Inspection reveals that $c\Gamma_{3+}$ corresponds to the antiferromagnetic structure observed in $FeF_3$ [19], $c\Gamma_{5+}$

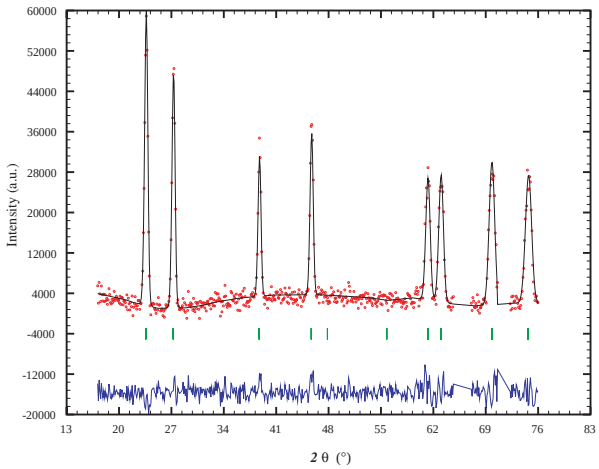


**Figure 2.** Fit to the magnetic diffraction pattern of $Gd_2Sn_2O_7$ obtained from the $\psi_6$ basis state by Rietveld refinement. The dots correspond to experimental data obtained by subtraction of that measured in the paramagnetic phase (1.4 K) from that in the magnetically ordered phase (0.1 K). The solid line corresponds to the theoretical prediction and the line below to the difference. Positions for the magnetic reflections are indicated by vertical markers.

to the linear combination observed in the model $XY$ pyrochlore antiferromagnet $Er_2Ti_2O_7$ [11], $c\Gamma_{7+}$ to the manifold of states proposed as the ground states for the Heisenberg pyrochlore antiferromagnet with dipolar terms (the PC ground state), and $c\Gamma_{9+}$ to a spin-ice like manifold observed in the non-collinear ferromagnetic pyrochlores such as $Dy_2Ti_2O_7$ [3]. While the phase transition in $Gd_2Sn_2O_7$ has been shown to be first order which allows ordering according to several irreducible corepresentations, it is commonly found that the terms which drive the transition to being first order are relatively weak and cause only minor perturbation to the resultant magnetic structure. Following this, we examined whether the models detailed above could fit the observed magnetic neutron diffraction spectrum. The goodness of fit parameter, $\chi^2$, for the fit to models characterised by each irreducible corepresentation are: $c\Gamma_{3+}$ (69.0), $c\Gamma_{5+}$ (35.6), $c\Gamma_{7+}$ (5.18), $c\Gamma_{9+}$ (13.6). We find that the magnetic scattering can only be well modeled by $c\Gamma_{7+}$, the PC state in which the moments of a given Gd tetrahedron are parallel to the tetrahedron's edges. In this state each moment is fixed to be perpendicular to the local 3-fold axis of each tetrahedron, consistent with Mössbauer data [13, 14]. Powder averaging leads to the structures ascribed to $\psi_4$, $\psi_5$ and $\psi_6$ being indistinguishable by neutron diffraction and prevents contributions of the individual basis vectors from being refined. For this reason only $\psi_6$ was used in the refinement and the final fit is presented in Figure 2. While the value of the ordered moment, 6(1) $\mu_B/Gd^{3+}$, obtained by scaling the magnetic and nuclear peaks is imprecise due to the uncertainty over the isotopic composition of the Gd and the concomitant neutron absorption, it is consistent with the free-ion value (7 $\mu_B$) and that measured by Mössbauer spectroscopy [13].

Realization of the PC state in $Gd_2Sn_2O_7$, but not in $Gd_2Ti_2O_7$, indicates that the magnetic Hamiltonian of the titanate contains additional terms. Cépas and Shastry [20] have suggested that next-neighbor exchange may stabilize magnetic ordering at $\mathbf{k} = (\frac{1}{2}\ \frac{1}{2}\ \frac{1}{2})$, though the corresponding region in the parameter space was found to be

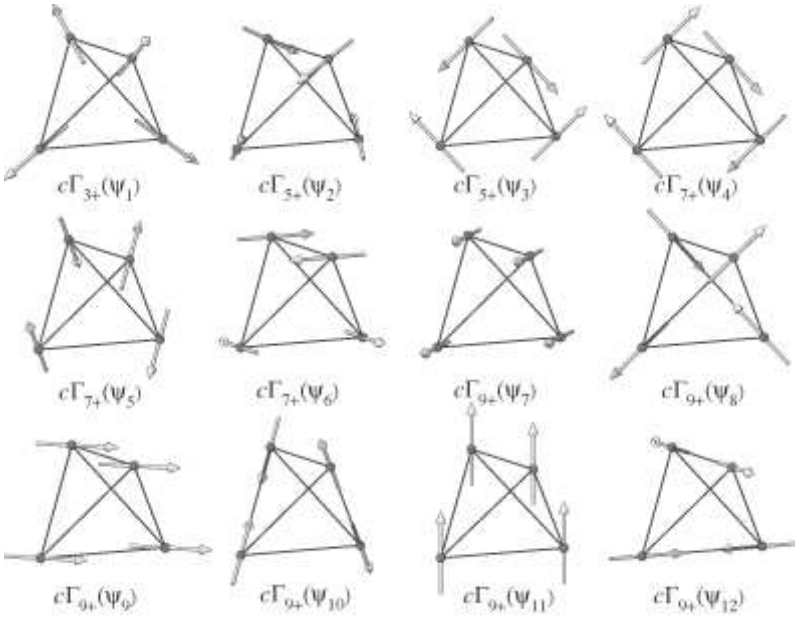


**Figure 3.** The magnetic structure basis vectors labelled according to the different irreducible corepresentations for $Gd_2Sn_2O_7$.

tiny. Also, possible exchange paths were not investigated in their work as both types of third-neighbor exchange (Fig. 1) were assumed to be equal.

The pyrochlore $A_2B_2O_7$ structure has two inequivalent oxygen sites: O1 at $(x, \frac{1}{8}, \frac{1}{8})$ and O2 at $(\frac{3}{8}, \frac{3}{8}, \frac{3}{8})$. The oxygen parameter is $x = 0.335$ and 0.326 for the stannate and the titanate, respectively [21]. Using this information we have determined that the nearest-neighbor gadolinium ions are connected with short Gd–O1(2)–Gd bonds. The second-neighbor exchange $J_2$ is produced by two distinct Gd–O1–O1–Gd bridges. The O1–O1 distance in the first path is 2.63 Å with two equal bond angles of 118°. In the second path, |O1–O1| = 3.04 Å, while the angles are 148° and 98°. (Distances and angles are given for $Gd_2Ti_2O_7$.)

There are two types of third-neighbour pairs in the pyrochlore lattice indicated in Fig. 1 as $J_{31}$ and $J_{32}$, which correspond to three- and two-step Manhattan (city-block) distances, respectively. The superexchange $J_{31}$ is determined by two equivalent Gd–O1–O1–Gd paths with |O1–O1| = 3.04 Å and two equal angles 148°. The superexchange $J_{32}$ is produced by two Gd–O1–O2–Gd bridges with a significantly larger interoxygen distance |O1–O2| = 3.62 Å and bond angles of 152° and 143°. As a result, the two exchange constants for third-neighbor pairs have to be different with $J_{32} \ll J_{31}$. The Goodenough-Kanamori-Anderson rules also suggest that the second-neighbor constant $J_2$ must be smaller than $J_{31}$ since bond angles in the corresponding superexchange paths are significantly closer to 90°. Similar relations should hold for next-neighbor exchange constants in $Gd_2Sn_2O_7$ with, perhaps, a somewhat larger ratio $J_2/J_{31}$ due to a larger angle 126° in the second-neighbor superexchange path. The overall effect of further neighbor exchange is, however, reduced in the stannate because of a larger lattice constant $a = 10.45$ Å compared to $a = 10.17$ Å in the titanate [21].

Next, we consider the following Hamiltonian

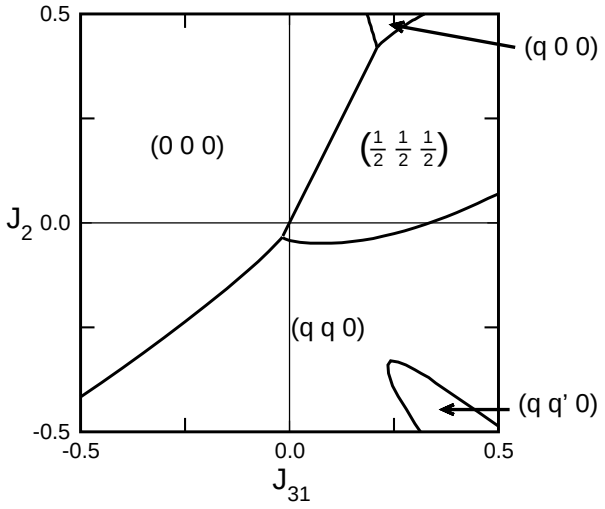


**Figure 4.** Instability wave-vectors for different values of second- and third-neighbor exchange constants for a Heisenberg pyrochlore antiferromagnet with dipolar interactions. Incommensurate states are indicated by nonzero components of the wave-vectors. All transition lines are of the first-order.

$$\hat{\mathcal{H}} = \sum_{\langle i,j \rangle} J_{ij} \mathbf{S}_i \cdot \mathbf{S}_j + D \sum_i (\mathbf{n}_i \cdot \mathbf{S}_i)^2 + (g\mu_B)^2 \sum_{\langle i,j \rangle} \Big[ \frac{\mathbf{S}_i \cdot \mathbf{S}_j}{r_{ij}^3} - \frac{3(\mathbf{S}_i \cdot \mathbf{r}_{ij})(\mathbf{S}_j \cdot \mathbf{r}_{ij})}{r_{ij}^5} \Big] \ ,$$

where the superexchange $J_{ij}$ extends up to the third-neighbor pairs of spins and $D > 0$ is a single-ion anisotropy. The strength of the dipolar interaction between nearest-neighbor spins $E_{dd} = (g\mu_B)^2/(a\sqrt{2}/4)^3$ is estimated as $E_{dd}/J \approx 0.2$ for the titanate [8], where $J$ is the nearest-neighbor exchange constant (in the following $J \equiv 1$). Applying mean-field theory [8, 20] and evaluating dipolar sums via the Ewald's summation we have determined the instability wave-vector for different values of second- and third-neighbor exchange constants. Results are essentially independent of the anisotropy constant $D > 0$ since the dipolar interaction already selects spins to be orthogonal to the local trigonal axes $\mathbf{n}_i$ for the eigenstates with the highest transition temperature.

If only the nearest-neighbor exchange is present, in agreement with previous works [8, 20] we find an approximate degeneracy of modes along the cube diagonal with a very shallow minimum $\sim 0.5\%$ at $\mathbf{k} = (\frac{1}{2}\,\frac{1}{2}\,\frac{1}{2})$. In such a case, a fluctuation driven first-order transition is expected to the PC state [9, 22]. The diagram of possible ordering wave-vectors for a restricted range of $J_{31}$ and $J_2$ are presented in Fig. 4. It contains two commensurate states with $\mathbf{k} = (0\,0\,0)$ and $\mathbf{k} = (\frac{1}{2}\,\frac{1}{2}\,\frac{1}{2})$ and three incommensurate phases. Remarkably, already weak *antiferromagnetic* $J_{31}$ robustly stabilizes the $\mathbf{k} = (\frac{1}{2}\,\frac{1}{2}\,\frac{1}{2})$ magnetic structure, which exists in a wide range $0 < J_{31} < 0.335J$. In contrast, a small *ferromagnetic* $J_2$ within a narrow window $-0.04J < J_2 < 0$is needed to obtain the same ordering without $J_{31}$. In the whole range of parameters, the eigenstate with $\mathbf{k} = (\frac{1}{2}\,\frac{1}{2}\,\frac{1}{2})$ corresponds to 120° spin structure with $q = 0$ in transverse kagomé plane with zero ordered moment on interstitial sites. The only remaining degeneracy corresponds to a four-fold orbit of $\mathbf{k} = (\frac{1}{2}\,\frac{1}{2}\,\frac{1}{2})$ vector.

We have also verified that the second type of third-neighbor exchange $J_{32}$ does not lead to further stabilization of the $(\frac{1}{2}\,\frac{1}{2}\,\frac{1}{2})$ spin structure. Based on these results and the above analysis of the exchange paths we conclude that it is the third-neighbor exchange across empty hexagons $J_{31}$ (Fig. 1), which is responsible for the magnetic structure observed in $Gd_2Ti_2O_7$ [11, 12]. In $Gd_2Sn_2O_7$ further neighbor exchanges play a less significant role due to a larger lattice constant and, in addition, the ratio $J_2/J_{31}$ might be enhanced due to somewhat different bond angles such that it lies closer to the transition boundary between $\mathbf{k} = (0\,0\,0)$ and $(\frac{1}{2}\,\frac{1}{2}\,\frac{1}{2})$ states.

In conclusion, the occurrence of the PC state in $Gd_2Sn_2O_7$ but not in $Gd_2Ti_2O_7$ indicates that the latter possesses additional contributions, which we identify as a type of third–neighbor exchange. $Gd_2Sn_2O_7$ presents, therefore, the only accurate realization of the Heisenberg pyrochlore antiferromagnet with dipolar interactions.

We are grateful to A. Forget for preparing the $^{160}$Gd enriched sample and to the ILL for provision of neutron time. ASW would like to thank the Royal Society and EPSRC (grant number EP/C534654) for financial support.

## References

[1] Anderson P W 1973 *Mat. Res. Bull.* **8** 153
[2] Villain J 1979 *Z. Phys.* B **33** 31
[3] Harris M J, Bramwell S T, McMorrow D F, Zeiske T and Godfrey K W 1997 *Phys. Rev. Lett.* **79** 2554
[4] Ballou R, Lelièvre-Berna E and Fåk B 1996 *Phys. Rev. Lett.* **77** 790
[5] Wills A S, Depuis V, Vincent E and Calemczuk R 2000 *Phys. Rev.* B **62** 9264(R)
[6] Urano C, Nohara M, Kondo S, Sakai F, Takagi H, Shiraki T and Okubo T 2000 *Phys. Rev. Lett.* **85** 1052
[7] Gingras M J P, den Hertog B C, Faucher M, Gardner J S, Dunsiger S R, Chang L J, Gaulin B D, Raju N P and Greedan J E 2000 *Phys. Rev.* B **62** 6496
[8] Raju N P, Dion M, Gingras M J P, Mason T E and Greedan J E 1999 *Phys. Rev.* B **59** 14489
[9] Palmer S E and Chalker J T 2000 *Phys. Rev.* B **62** 488
[10] Glazkov V N, Zhitomirsky M E, Smirnov A I, Krug von Nidda H-A, Loidl A, Marin C and Sanchez J P 2005 *Phys. Rev.* B **72** 020409(R); Glazkov V N, Smirnov A I, Sanchez J P, Forget A, Colson D and Bonville P 2005 *Preprint* cond-mat/0510575
[11] Champion J D M, Wills A S, Fennell T, Bramwell S T, Gardner J S and Green M A 2001 *Phys. Rev.* B **64** 140407
[12] Stewart J R, Ehlers G, Wills A S, Bramwell S T and Gardner J S 2004 *J. Phys.: Condens. Matter* **16** L321
[13] Bonville P, Hodges J A, Ocio M, Sanchez J P, Vulliet P., Sosin S and Braithwaite D 2003 *J. Phys. Condens. Matter.* **15** 7777
[14] Bertin E, Bonville P, Bouchaud J-P, Hodges J A, Sanchez J P and Vulliet P 2002 *Eur. Phys. J.* B **27** 347
[15] Wills A S 2000 *Physica* B **276** 680; progam available from ftp.ill.fr/pub/dif/sarah/
[16] Rodriguez-Carvajal J 1993 *Physica B* **192** 55
[17] Kovalev O V 1993 *Representations of the Crystallographic Space Groups* Edition 2 (Gordon and Breach Science Publishers, Switzerland)
[18] The corepresentations are real and are labelled according to the notation of Kovalev [17] for the parent representation and whether the antiunitary halfing group was created according to the $d(a) = \pm\delta(aa_0^{-1})\beta$, where $d(a)$ is the matrix representitive of antiunitary symmetry element $a$, $\delta(aa_0^{-1})$ is the matrix representitive of unitary symmetry element $aa_0^{-1}$, $a_0$ is an antiunitatry generating element and $\beta$ is an unitary matrix.
[19] Greedan J E, O'Reilly A H and Stager C V 1987 *Phys. Rev.* B **35** 8770
[20] Cépas O. and Shastry B. M. 2004 *Phys. Rev.* B **69** 184402
[21] Kennedy B J, Hunter B A and Howard C J 1997 *J. Solid State Chem.* **130** 58; Helean K B, Ushakov S V, Brown C E, Navrotsky A, Lian J, Ewing R C, Farmer J M and Boatner L A 2004 *ibid*. **177** 1858
[22] Brazovskii S A 1975 Zh. Éksp. Teor. Fiz. **68**, 175 [Sov. Phys. JETP **41** 85]; Cepas O, Young A P and Shastry B S 2005 Phys. Rev. B **72** 184408